

# Photodissociation of OCS at 222 nm. The triplet channel

G. Nan<sup>1</sup>, I. Burak<sup>2</sup> and P.L. Houston

*Department of Chemistry, Cornell University, Ithaca, NY 14853-1301, USA*

Received 8 March 1993; in final form 10 May 1993

The dissociation of OCS at 222 nm produces both S(<sup>1</sup>D) and S(<sup>3</sup>P). By monitoring the Doppler profile of the minor S(<sup>3</sup>P<sub>2</sub>) product on the <sup>3</sup>D<sub>3/2</sub>←<sup>3</sup>P<sub>2</sub> transition it is determined that the branching ratio for this triplet channel is 5% relative to the singlet channel. Detailed analysis of the Doppler profiles provides an anisotropy parameter of  $\beta=0.3\pm 0.2$  and a recoil speed distribution whose average energy is 37% of the 19881 cm<sup>-1</sup> available energy. The remainder of the energy, 12525 cm<sup>-1</sup>, is deposited into CO vibration and rotation. The distributions for both the relative translation and the CO internal energy are broad.

## 1. Introduction

The dynamics of photodissociation events give substantial insight into the potential energy surfaces for excited molecules. For spin-allowed processes, the dissociation often occurs on a single surface, so that a measurement of the translational and internal energy distributions of the products can be used to estimate how the bond angles and lengths change along the trajectory representing dissociation on the potential surface. For spin-forbidden processes, more than one surface is typically important, and the dynamics of the dissociation can often provide clues as to the coupling between them. In this Letter, we examine the spin-forbidden dissociation of OCS to CO and S(<sup>3</sup>P).

Previous experiments on photodissociation of OCS at 222 nm in this laboratory [1] measured the branching ratio between the S(<sup>1</sup>D) and S(<sup>3</sup>P<sub>2</sub>) channels and concluded that the triplet channel is negligible; an upper limit of 2% was determined for the quantum yield. The singlet channel gave CO with little vibrational excitation but with large rotational excitation. The CO population had a maximum at  $J=55$  and secondary maximum at  $J=67$ . The an-

isotropy associated with  $J=67$  rotational level was characterized by  $\beta=1.9$ , while that associated with  $J=55$  was zero. These observations were interpreted by a model in which the dissociation takes place through excitation to both A' and A'' Renner-Teller components of the <sup>1</sup>Δ state; the lower A' state is bent with the transition dipole parallel to the C-S bond, while the upper A'' state has a dipole moment perpendicular to the OCS molecular plane. Since the CO bond is relatively unaffected by the dissociation, little vibrational excitation was observed in the CO photofragment.

More recently, Nan et al. studied the E→V, R, T transfer to small molecules from S(<sup>1</sup>D) produced from 222 nm photodissociation of OCS [2]. These more sensitive experiments measured the Doppler profiles of the S(<sup>3</sup>P<sub>2</sub>) as a function of time for fixed pressures of the quenching gas following the photolysis of OCS at 222 nm. In contrast to the results of Sivakumar et al., who did not observe triplet sulfur produced in the 222 nm photolysis [1], Nan et al. observed S(<sup>3</sup>P<sub>2</sub>) shortly after the photolysis under collision-free conditions without added quencher molecules. In this Letter, we report the branching ratio for the triplet channel, the recoil anisotropy, and the partitioning of the excess photolysis energy into relative translation as determined by a study of the Doppler profile of the S(<sup>3</sup>P<sub>2</sub>) product.

<sup>1</sup> Current address: No 8, Building 23, Yui-jin Li, Copng-tai Dr., Handan, Hebei Province 056004, People's Republic of China.

<sup>2</sup> Permanent address: School of Chemistry, Tel Aviv University, Tel Aviv, Israel.

## 2. Experimental

The experimental setup was similar to that described previously [2]. A low-pressure OCS sample (a few mTorr) was placed in a glass cell and photolyzed with pulsed 222 nm light. Shortly after the dissociation, the triplet sulfur product  $S(^3P_2)$  was monitored through its Doppler profile measured by laser-induced fluorescence (LIF) on the transition  $S(^3D_3) \leftarrow S(^3P_2)$  at  $67843 \text{ cm}^{-1}$  (147 nm). When the OCS was diluted in mixtures with CO, the integrated intensity of the  $S(^3P_2)$  Doppler profile increased due to quenching of  $S(^1D)$ , and the increase could be measured as a function of the time delay between the photolysis and the probe pulses.

The pulsed 222 nm photolysis light was generated by a Nd:YAG (Quanta-Ray, DCR-2A) pumped dye laser (PDL-2) system. The doubled Nd:YAG output at 532 nm, with typical power of 560 mJ/pulse, pumped the dye laser with rhodamine 590 tuned to 561 nm, generating a power of around 100 mJ/pulse. The 222 nm light was generated by summing the Nd:YAG 1064 nm fundamental with the doubled output from the dye laser at 280.5 nm. The usual power at 222 nm was 2 mJ/pulse, and the pulse length was 6 ns. The laser output was polarized in the horizontal plane and could be rotated with a double Fresnel rhomb (Karl Lambrecht). The laser beam was collimated to a diameter of around 3 mm before entering the sample cell. In order to normalize the LIF signals, a photodiode monitored the fluorescence from a cuvette of dye solution after the beam exited the cell.

The Doppler profile measurement of  $S(^3P_2)$  on the  $^3D_3 \leftarrow ^3P_2$  transition was performed with VUV light at 147 nm generated by four-wave sum mixing in magnesium vapor [1]. Two dye lasers (Lambda Physik FL2000E), pumped by one XeCl excimer laser (Lambda Physik LPX200) through a beam splitter with an adjustable reflection/transmission ratio, provided the electronic excitation in the magnesium vapor. The polarization of the one dye laser output was rotated by  $90^\circ$  with a half-wave plate from its original orientation. The two laser beams were then spatially combined in a Glan-Taylor prism and then passed through a quarter-wave plate so that they became circularly polarized in opposite directions. The beams were then focused into the center of the

magnesium heat pipe. Both dye lasers were equipped with air-spaced intracavity etalons. The dye laser wavelength for the two-photon transition ( $3s3d \ ^1D \leftarrow 3s^2 \ ^1S$ ) in Mg was fixed at 430.9 nm, with power of about 4 mJ/pulse. To produce the 147 nm VUV light for scanning the  $S(^3P)$  profile, the second laser at 466.2 nm was tuned by ramping the pressure of  $N_2$  in the grating/etalon housing. The pulse energy of the line-narrowed 466.2 nm light was typically 10 mJ. The pulse duration for each dye laser was approximately 15 ns. The etalon-narrowed VUV linewidth was  $0.14 \text{ cm}^{-1}$  fwhm.

The photolysis beam and the probe beam entered the sample cell at right angles to one another (a detailed description of the cell can be found in ref. [2]). The entrance and the exit windows for the 222 nm photolysis light were  $S_1$ -UV quartz flats. Lithium fluoride windows were used for the entrance and exit of the VUV probe beam. The laser-induced fluorescence was monitored through a LiF window mounted on top of the cell. The intersection region of the two laser beams was very close to the fluorescence detection window so as to decrease the absorption of fluorescence by OCS. The cell was large (75 mm diameter and 200 mm high) and the path length of the photolysis laser was short (100 mm from the entrance window on one arm to the exit window on the other arm) so as to reduce the pressure of accumulated products. The samples were introduced into the cell from one of two teflon stopcocks at the bottom of the cell. The pressure was monitored at the other stopcock and also at the entrance stopcock using two capacitance manometers. A 100 Torr full scale manometer (MKS221) was used at the entrance of the cell and a 1 Torr full scale manometer (MKS310) was connected to the cell through the teflon stopcock.

The LIF signal was detected by a solar-blind photomultiplier (EMR 542G-09-17) with a 40 mm f/1 imaging lens at the top window on the cell. The region from the window to the cathode of the PMT was evacuated to transmit the VUV fluorescence light. Signals were averaged in boxcar integrators (Stanford SRS-250) and collected by an LSI-11 computer.

The timing of the laser pulses was controlled by a digital delay/pulse generator (SRS DG535) operating at a master frequency of 10 Hz.

OCS was obtained from Matheson in a lecture bot-

tle and further purified with freeze-pump-thaw cycles. CO was also obtained from Matheson and used without further purification.

### 3. Results

The intensity of the  $S(^3P_2)$  Doppler profile in the 222 nm photolysis of a dilute mixture of OCS in CO increases with the delay time between the photolysis and the probe pulses from a delay corresponding to zero collisions to a delay corresponding to one collision. Fig. 1 displays the  $S(^3P_2)$  Doppler profiles measured from photolysis 5 mTorr of OCS in 55 mTorr of CO at four delay times between the two lasers and for a polarization of the photolysis laser parallel with respect to the propagation direction of the probe laser. The profile measured at a 50 ns delay is identical to that measured from 5 mTorr OCS alone at the same delay. At this pressure and time delay the average number of interparticle collisions is much less than one, so the contribution to the  $S(^3P_2)$  intensity from quenching of  $S(^1D)$  by CO is negligible and by OCS is small. Thus, the measured  $S(^3P_2)$  is from a channel of direct OCS photodissociation at 222 nm.

Fig. 2 shows the measured  $S(^3P_2)$  Doppler pro-

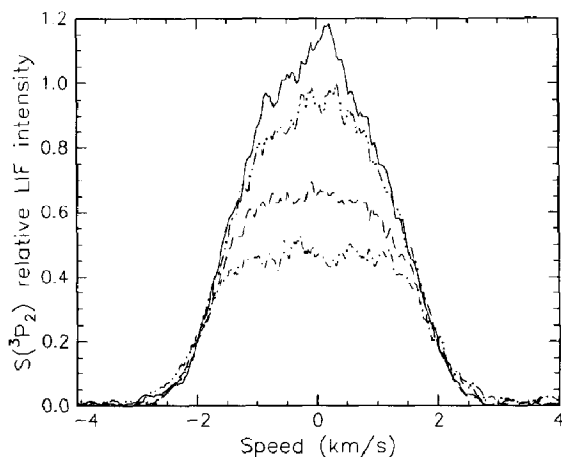


Fig. 1. Doppler profiles of  $S(^3P_2)$  following photolysis of a mixture of 5 mTorr of OCS and 55 mTorr of CO as a function of the delay time between the photolysis and probe pulses for parallel polarization. (—) 450 ns; (···) 300 ns; (---) 150 ns; (-·-·) 50 ns.

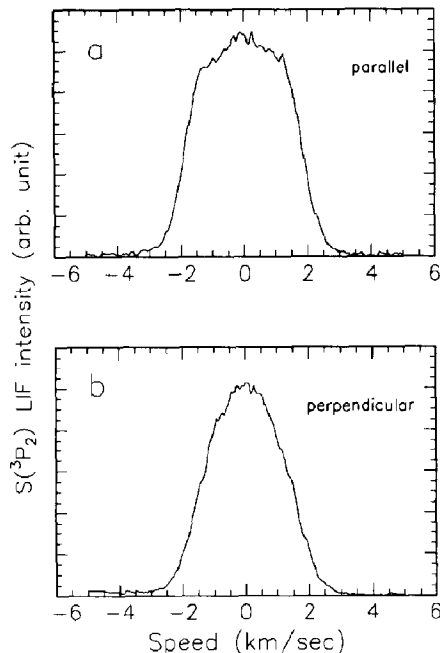


Fig. 2.  $S(^3P_2)$  Doppler profiles measured at 80 ns after photolysis 10 mTorr of OCS. The electric vector of the photolysis laser was (a) parallel and (b) perpendicular to the propagation direction of the probe laser.

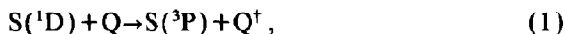
files 80 ns after photolysis of 10 mTorr of OCS at 222 nm. Fig. 2a was measured with the electric field vector of the photolysis laser parallel to the propagation direction of the probe laser, while fig. 2b was measured with perpendicular polarization. There are clear differences between the Doppler profiles measured using the different polarizations. That measured in the parallel configuration has more sharply sloped sides and a wider half-width than that measured in the perpendicular configuration. However, as discussed below, the profiles are not consistent with one another, in that the anisotropy determined from one profile cannot reproduce the other. The reason is that, even at 10 mTorr, there is a small amount of quenching of  $S(^1D)$  by the OCS.

### 4. Discussion

#### 4.1. The quantum yield of $S(^3P_2)$ in 222 nm dissociation of OCS

As the number of collisions between the sulfur and the quenching molecules increases, either with in-

creasing pressure of the quenching molecule or with increasing time delay between the photolysis and probe pulses, the concentration of  $S(^3P_2)$  increases as a result of electronic relaxation of  $S(^1D)$ ,



where  $Q$  represents a quencher molecule and  $^\dagger$  indicates excitation in vibration, rotation and/or translation. When the pressure of OCS is much smaller than that of the quencher molecule, as was the case in our experiment,  $[S(^1D)]_0 \ll [Q]$  and eq. (1) is pseudo-first order with respect to  $S(^1D)$ ,

$$[S(^1D)] = [S(^1D)]_0 \exp(-\sum k_i [Q_i] t), \quad (2)$$

where  $k_i$  is the quenching rate constant for the quencher  $Q_i$  and for CO is  $k = 6.3 \times 10^{-11} \text{ cm}^3 \text{ mol}^{-1} \text{ s}^{-1}$  as measured in our experiment. Quenching due to the small pressure of OCS was also taken into account, with  $k = 1.5 \times 10^{-10} \text{ cm}^3 \text{ mol}^{-1} \text{ s}^{-1}$ , as measured by Black and Jusinski [3].

From eq. (2), the concentration of triplet sulfur produced by quenching,  $[S(^3P_2)]_q$ , can be expressed as

$$[S(^3P_2)]_q = a[S(^1D)]_0 \times \left[ 1 - \exp\left(-\sum k_i [Q_i] t\right) \right], \quad (3)$$

where  $a$  represents the branching ratio of  $S(^3P_2)$  from quenching  $S(^1D)$ , and has been assumed to be the same for CO and OCS. In the following calculation of the  $S(^3P_2)$  quantum yield from direct OCS dissociation,  $a = 0.8$  is used for both CO and OCS. This value was found by McBane et al. for quenching of  $S(^1D)$  by nitrogen [4].

At any time delay  $t$  the  $S(^3P_2)$  concentration is the sum of the concentration produced by photolysis and the concentration produced by quenching,

$$\begin{aligned} [S(^3P_2)] &= [S(^3P_2)]_0 + [S(^3P_2)]_q, \\ [S(^3P_2)] &= [S(^3P_2)]_0 = a[S(^1D)]_0 \\ &\times \left[ 1 - \exp\left(-\sum k_i [Q_i] t\right) \right]. \end{aligned} \quad (4)$$

The branching ratio  $[S(^3P_2)]_0/[S(^1D)]_0$  can be determined from the Doppler profile intensity, given the quenching rates  $k_i$  and the quencher concentra-

tions  $[Q_i]$ , by fitting eq. (4) at several delay times and assuming that the concentration  $[S(^3P_2)]$  is proportional to the integrated intensity of the Doppler profiles.

Fig. 3 plots the integrated  $S(^3P_2)$  Doppler profile intensity as a function of  $t$  for the data in fig. 1 from photolysis 5 mTorr of OCS in 55 mTorr of CO and  $t$  from 50 to 450 ns. The dashed line is an exponential fit in the form of eq. (4) with the following parameters:  $k_{CO} = 6.3 \times 10^{-11} \text{ cm}^3 \text{ mol}^{-1} \text{ s}^{-1}$ ,  $[CO] \approx 1.78 \times 10^{15} \text{ mol/cm}^3$ ,  $k_{OCS} = 1.5 \times 10^{-10} \text{ cm}^3 \text{ mol}^{-1} \text{ s}^{-1}$ , and  $[OCS] \approx 1.62 \times 10^{14} \text{ mol/cm}^3$ . The ratio  $[S(^3P_2)]_0/a[S(^1D)]_0$  is measured as 0.065. With  $a = 0.8$ , the branching ratio for  $S(^3P_2)$  from direct dissociation is 5%. The quantum yields for the other triplet states,  $S(^3P_1)$  and  $S(^3P_0)$ , have not been measured but, when included, would make the total quantum yield for the triplet channel larger. If OCS photolysis were to produce triplet states with a room temperature statistical population, the quantum yield for the triplet channel would increase to 5.5%.

The photolysis of OCS at 222 nm thus has a small branching ratio for the triplet  $S(^3P_2)$  which, assuming  $a = 0.8$ , is measured to be larger than in the previous report [1], where an upper limit for the  $S(^3P_2)$  quantum yield of 2% was measured.

It is interesting to compare our result for the triplet quantum yield in the OCS photodissociation at 222 nm (about 5.5%) to that for the triplet yield in

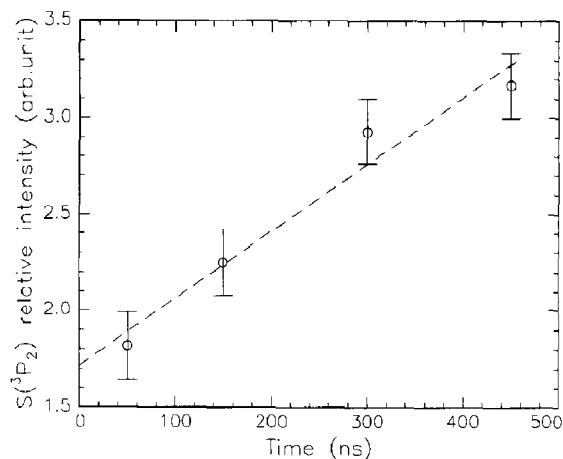


Fig. 3. The relative  $S(^3P_2)$  concentration (obtained from integrating the Doppler profiles) as a function of time (O). (---) exponential fit described in the text.

CO<sub>2</sub> photodissociation at 157 nm. The two molecules are isoelectronic, and excitation at these respective wavelengths excites each molecule to the same dissociative <sup>1</sup>Δ state. In the case of CO<sub>2</sub>, Zhu and Gordon [5], who used a quenching technique, found that the yield of O(<sup>3</sup>P) was 6%, while Stolow and Lee [6], using molecular beam time-of-flight analysis, found (6±2)%. It thus appears that the triplet yields for dissociation of OCS and CO<sub>2</sub> through these similar states are comparable. On the other hand, the percentage of available energy deposited into translation and the anisotropy values seem to be different: 58% and β=2.0 for CO<sub>2</sub> [7], versus 37% and β=0.3 for OCS (see below).

#### 4.2. OCS 222 nm photofragmentation dynamics for the triplet channel

The S(<sup>3</sup>P<sub>2</sub>) Doppler profiles shown in fig. 2 exhibit considerable differences between measurements made with parallel and perpendicular polarization of the photolysis laser relative to the propagation direction of the probe laser. Thus, the lifetime of the excited dissociative state must be short compared with its rotation period. Since the photofragments recoil in the axial direction for thermal rotational energies of the OCS molecule, the observation in fig. 2 of a wider profile in the parallel configuration versus the perpendicular one indicates qualitatively that the transition dipole in OCS is more nearly parallel to the molecular axis.

In principle, an accurate determination of the anisotropy in the sulfur velocity distribution can be obtained from Doppler profiles measured for both the parallel and the perpendicular configurations. If the dissociation is rapid compared to parent molecular rotation and if the anisotropy is independent of the speed, then the Doppler profile should be given by [8,9]

$$F(v, \theta) = [1 + \beta P_2(\cos \theta)] f(v) / 4\pi, \quad (5)$$

where  $f(v)$  is the speed distribution (discussed below),  $\theta$  is the angle between the polarization direction of the photolysis light and the propagation direction of the probe laser,  $P_2$  is the second-order Legendre polynomial, and the anisotropy parameter  $\beta$  equals  $2P_2(\cos \chi)$ , where  $\chi$  is the angle between the transition moment and the fragment recoil direc-

tion. Ideally, the same value of  $\beta$  and the same distribution  $f(v)$  should fit both parallel and perpendicular measurements with  $\theta=0^\circ$  and  $\theta=90^\circ$ , respectively. However, the Doppler profile measured with parallel polarization in our experiment tends to give a smaller  $\beta$  than that measured with perpendicular polarization. A likely complication is that the Doppler profiles of fig. 2 could contain a small contribution from relaxation of S(<sup>1</sup>D) by OCS, which would tend to give a Gaussian-like contribution to both profiles.

An estimate of the size of this quenching effect can be made from the OCS pressure of 10 mTorr, the quenching rate of S(<sup>1</sup>D) by OCS,  $1.5 \times 10^{-10} \text{ cm}^3 \text{ mol}^{-1} \text{ s}^{-1}$ , the time delay of 80 ns, and the branching ratio for S(<sup>3</sup>P<sub>2</sub>) production of 5%. At this pressure and time delay there are 0.004 quenching collisions of S(<sup>1</sup>D) by OCS. While this quenching produces a negligible effect on the S(<sup>1</sup>D) quantum yield, the triplet yield, being 20 times less than the singlet yield, is affected 20 times more. Thus, the yield of triplet from quenching is  $0.004 \times 20 = 0.08$  of the yield in the absence of quenching. Consequently, we might expect that about 8% of the integrated intensities for the profiles in fig. 2 is due to quenching. If we assume that quenching produces a velocity distribution giving rise to a Gaussian contribution to the profiles, we can subtract the quenching contribution to see if the remaining profiles are consistent with one another.

Fig. 4 presents such an analysis. The solid line shows the data of figs. 2a and 2b after subtraction from each of a Gaussian whose width was adjusted to provide reasonable resulting profiles and whose integrated intensity was taken to be 8% of the total (the Gaussian is shown as a dash-dot line). The resulting profiles (solid lines) were then fit by a function of the form given in eq. (5) using same speed distribution function (see below) and the same value of  $\beta=0.3$  for the two configurations. The results, which provide an excellent fit to the corrected data, are shown as dashed lines. The analysis gives an anisotropy parameter of  $\beta=0.3 \pm 0.2$ , where the uncertainty comes primarily from the uncertainty in the assumed width of the Gaussian.

The speed distribution used in the fit can be used to determine the distribution of energy in fragment recoil, or equivalently the internal energy distribu-

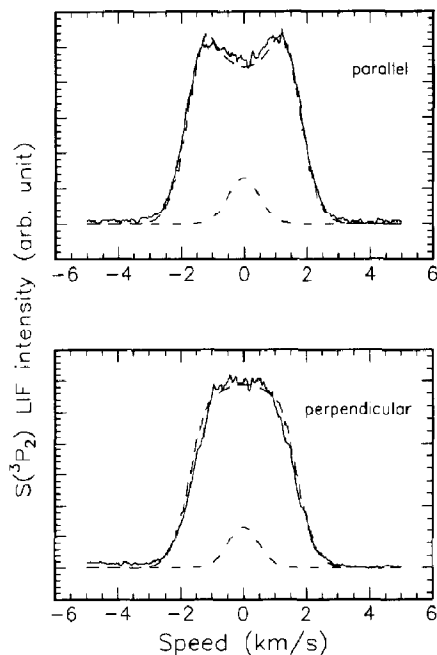


Fig. 4. Analysis of the data of fig. 2. A Gaussian (---) was subtracted from each of the data sets of fig. 2 to account for quenching of  $S(^1D)$  by OCS, and the resulting profiles (—) were fit to a function of the form given by eq. (6) of the text. From the fit (-.-), a value of  $\beta=0.3\pm 0.2$  was determined for the anisotropy parameter.

tion of the CO fragment. The calculated Doppler profile is very sensitive to both the first moment (the average speed) and the second moment (the width) of the speed distribution. The corrected Doppler profiles of fig. 4 were fit with a speed distribution function of the form

$$f(v) = 0, \quad v < v_s,$$

$$f(v) \propto (v - v_s)^2 \exp\left(-\frac{m_{\text{OCS}}(v - v_s)^2}{2kT}\right), \quad v \geq v_s,$$
(6)

where  $m_{\text{OCS}}$  is the OCS mass,  $T=3000$  K, and  $v_s=900$  m/s. This distribution gives an average laboratory frame  $S(^3P_2)$  velocity of  $v_{s,\text{lab}}=1929$  m/s. The c.m. sulfur velocity,  $v_{s,\text{c.m.}}$ , can be obtained by deconvoluting the OCS thermal velocity, but it can also simply be approximated by subtracting the average thermal speed of OCS from  $v_{s,\text{lab}}$ . The relative recoil velocity between CO and  $S(^3P_2)$  is  $(m_{\text{OCS}}/m_{\text{CO}})v_{s,\text{c.m.}}$  and corresponds to 37% of the ex-

cess photolysis energy,  $E_{\text{photon}} - D_0 = 45045 - 25164 \text{ cm}^{-1} = 19881 \text{ cm}^{-1}$ , where  $D_0$  is the dissociation energy (ref. [123] in ref. [1]). It is thus concluded that 63% of the excess photolysis energy, or  $12525 \text{ cm}^{-1}$ , is in the form of CO vibration and rotation. The speed distribution used in fitting the measured Doppler profiles (fig. 4) is very broad ( $T=3000$  K), indicating that the internal energy in the CO fragment also has a broad distribution.

While it is not yet possible with the results of this experiment to make a detailed comparison between the dynamics of the singlet and triplet channels, the results obtained here suggest that the two channels may be quite similar. Both channels, when averaged over final states, produce fragments with an anisotropy characterized by a positive value of  $\beta$ . In fact, the profiles shown here for  $S(^3P_2)$  in fig. 4 are very similar in shape to those of ref. [1], fig. 8 for  $S(^1D)$ . Both channels produce CO in a broad distribution with about 60% of the available energy in internal degrees of freedom. In the singlet channel, the energy is almost all in rotation, and it is possible, though not yet proven, that the triplet channel also populates high CO rotational states. If further experiments confirm that the two channels have similar dynamics, it would suggest that the crossing from the originally excited singlet state to the triplet state occurs after most of the available energy has been partitioned into the final degrees of freedom.

## 5. Conclusion

The triplet  $S(^3P_2)$  channel in photodissociation of OCS at 222 nm has been studied with Doppler spectroscopy on the  $^3D_3 \leftarrow ^3P_2$  transition of  $S(^3P_2)$ . The branching ratio for this triplet channel was measured as 5% relative to the singlet channel.

The excited state lifetime of the OCS at this wavelength (222 nm) is short compared to its rotation period. An anisotropy parameter  $\beta=0.3\pm 0.2$  indicates that the transition moment is predominantly parallel to the OCS axis.

An average of 37% of the  $19881 \text{ cm}^{-1}$  excess photolysis energy is deposited into the relative recoil of the photofragments, with the rest of the energy going to the vibration and rotation of the CO molecules.

The distributions for both the relative translation and the CO internal energy are broad.

### References

- [1] N. Sivakumar, G.E. Hall, P.L. Houston, I. Burak and J.W. Hepburn, *J. Chem. Phys.* **88** (1988) 3692.
- [2] G. Nan, D.W. Neyer, P.L. Houston and I. Burak, *J. Chem. Phys.*, accepted for publication.
- [3] G. Black and L.E. Jusinski, *J. Chem. Phys.* **82** (1985) 789.
- [4] G.C. McBane, I. Burak, G.E. Hall and P.L. Houston, *J. Phys. Chem.* **96** (1992) 753.
- [5] Y.F. Zhu and R.J. Gordon, *J. Chem. Phys.* **92** (1990) 2897.
- [6] A. Stolow and Y.T. Lee, *J. Chem. Phys.* **98** (1993) 2066.
- [7] Y. Matsumi, N. Shafer, K. Tonokura, M. Kawasaki, Y.-L. Huang and R.J. Gordon, *J. Chem. Phys.* **95** (1991) 7311.
- [8] R.N. Zare and D.R. Herschbach, *Proc. IEEE* **51** (1963) 173.
- [9] R. Schmiedl, H. Dugan, W. Meier and K.H. Welge, *Z. Physik A* **304** (1982) 137.